REPORT DOCUMENTATION PAGE

Form Approved
OMB No. 0704-0188

1. AGENCY USE ONLY *(Leave blank)*	2. REPORT DATE	3. REPORT TYPE AND DATES COVERED
	26 JAN 04	FINAL REPORT JULY 2003

4. TITLE AND SUBTITLE
THE EFFECTS OF ADHESION AND NANO-STRUCTURE ON THE TOUGHNESS OF POLYMER NANO-COMPOSITES

5. FUNDING NUMBERS
9270-CH-01
N62558-02-M-5603

6. AUTHOR(S)
A.J. KINLOCH
A.C. TAYLOR

7. PERFORMING ORGANIZATION NAME(S) AND ADDRESS(ES)
IMPERIAL COLLEGE OF SCIENCE TECHNOLOGY & MEDICINE
DEPARTMENT OF MECHANICAL ENGINEERING
EXHIBITION ROAD
LONDON SW7 2BX
UNITED KINGDOM

8. PERFORMING ORGANIZATION REPORT NUMBER

9. SPONSORING / MONITORING AGENCY NAME(S) AND ADDRESS(ES)
U.S. ARMY - EUROPEAN RESEARCH OFFICE
EDISON HOUSE
223 OLD MARYLEBONE ROAD
LONDON NW1 5TH
UNITED KINGDOM

10. SPONSORING / MONITORING AGENCY REPORT NUMBER

11. SUPPLEMENTARY NOTES

12a. DISTRIBUTION / AVAILABILITY STATEMENT
APPROVED FOR PUBLIC DISTRIBUTION
DISTRIBUTION UNLIMITED
RINAL REPORT

12b. DISTRIBUTION CODE

13. ABSTRACT *(Maximum 200 words)*

14. SUBJECT TERMS
ADHESION, NANO-STRUCTURE, POLYMER NANO-COMPOSITES

15. NUMBER OF PAGES
32

16. PRICE CODE

17. SECURITY CLASSIFICATION OF REPORT	18. SECURITY CLASSIFICATION OF THIS PAGE	19. SECURITY CLASSIFICATION OF ABSTRACT	20. LIMITATION OF ABSTRACT
UNCLASSIFIED	UNCLASSIFIED	UNCLASSIFIED	

THE EFFECTS OF ADHESION AND NANO-STRUCTURE ON THE TOUGHNESS OF POLYMER NANO-COMPOSITES

FINAL REPORT, JULY 2003

UNITED STATES ARMY

EUROPEAN RESEARCH OFFICE OF THE U.S. ARMY

LONDON, ENGLAND

CONTRACT NUMBER N62558-02-M-5603

A.J. KINLOCH & A.C. TAYLOR

IMPERIAL COLLEGE, LONDON, UK

Abstract

Epoxy nanocomposites have been manufactured using a range of modifiers, including organoclays, silica nanoparticles, carbon nanotubes and carbon nanofibres. The mechanical and fracture properties of these materials have been investigated, and the structure/property relationships discussed. Modelling methods have been used to predict the performance of these materials.

Epoxy micro- and nano-composites have been manufactured using a range of inorganic modifiers, with exfoliated, intercalated and particulate morphologies. Indeed, by changing the surface treatment, and hence the interfacial adhesion, the type of morphology obtained could be varied. The modulus and fracture toughness of these composites increased with the weight fraction of modifier. The fracture toughness was increased by up to 150% with the addition of mica, but the material modified with the surface-treated clays generally showed only a small toughening effect. The modulii of the composites were in good agreement with predictions using the van-Es-modified Halpin-Tsai model. The fracture toughness of the clay-modified materials generally decreased as the degree of exfoliation increased, as the modifier acts like large particles rather than individual platelets, hence having a lower effective aspect ratio and a smaller toughening effect. The nanocomposites tend to behave in a similar manner to the microcomposites, and the same models can be applied to describe the performance of these systems.

The addition of low concentrations of nano-silica (SiO_2) particles to a typical rubber-toughened adhesive, based upon a two-part epoxy formulation, leads to very significant increases in the toughness of the adhesive, and also to increases in the glass transition temperature and the single-lap shear strength. The nano-SiO_2 particles have an average particle diameter of 20 nm and are very well dispersed in the epoxy adhesive. They were surface treated, via using an added silane-coupling agent, to give excellent interfacial adhesion to the epoxy matrix. Only a concentration of about 1% to 8 % by mass of such nano-particles are needed to achieve significant improvements in the mechanical and thermal performance of the rubber-toughened two-part epoxy adhesive. These novel results represent the first report of nano-particles significantly increasing the toughness of thermosetting polymers.

Two structural epoxy adhesives have been formulated to investigate the toughening effect of carbon nanotubes and nanofibres. These are a low-viscosity resin and a hot-melt formulation. The viscosity and handleability of both these systems are excellent. The addition of 2% by mass of multi-walled carbon nanotubes to the hot-melt epoxy gave no significant increase in the mean initiation fracture energy, but the carbon nanofibres do give a significant toughening effect, the mean initiation value of G_c increasing by 25% to 160 J/m^2.

Two different methods of modelling the performance of particulate composites using the finite element method have started to be investigated. The methodologies have been initially verified by applying these methods to an epoxy adhesive filled with hollow, spherical, glass beads. The agreement between the theoretical predictions of the stress versus strain response and the experimental data is good. The models predict the formation of shear bands within the epoxy matrix, and confirm the experimental observations that there is little or no adhesion between the hollow glass spheres and the epoxy matrix.

Contents

1. Introduction

There are many advantages that polymeric adhesives can offer compared to the more traditional methods of joining such as bolting, brazing, welding, mechanical fasteners, etc. These include [1, 2] the ability to join dissimilar materials to give light-weight, but strong and stiff structures, such as honeycomb sandwich panels. Also, polymeric adhesives may be used to join thin-sheet material efficiently which, due to its low bearing strength, cannot be readily joined by other methods. Further, adhesive bonding frequently represents the most convenient and cost-effective joining technique and, indeed, the bonding operation can often be readily automated. For these reasons, adhesive bonding is widely used in many industries, for example in the automobile, truck, aerospace, railway and electronic industries. Epoxy adhesives represent the most common type of *structural* adhesive; the term *structural* meaning that the polymerised (i.e. cured or hardened) adhesive possesses a relatively high modulus and strength so that a load-bearing joint is formed.

When polymerised, epoxy adhesives are amorphous and highly-crosslinked (i.e. thermosetting) materials. This microstructure results in many useful properties for structural engineering applications, such as a high modulus and failure strength, low creep, and good performance at elevated temperatures. However, the structure of such thermosetting polymers also leads to one highly undesirable property in that they are relatively brittle materials, with a poor resistance to crack initiation and growth.

The present report discusses the effects of using novel, nano-scale, toughening approaches to increase the toughness of these brittle materials without degrading the other properties. These are firstly the use of inorganic silicates (i.e. clays) where the surface properties have been modified to change the degree of interfacial adhesion to the matrix, secondly the addition of silica nanoparticles, and thirdly the use of carbon nanotubes and carbon nanofibres. In addition, modelling of these particle-modified materials will be discussed.

2. Mechanical and Fracture Properties of Epoxy/Inorganic Micro- and Nano-composites

2.1. Introduction

In recent years the concept of forming hybrids using polymers and inorganic materials has received a significant amount of attention. Many of these studies have used surface-treated silicates, or organoclays, to produce layered-silicate nano-composites, e.g. [3, 4]. A nano-composite is defined as a composite where one of the components has a dimension in the nanometre range. Many claims for the potential of these organic/inorganic hybrids have been made, but for some important combinations of materials little experimental data has been produced. For example, the addition of inorganic filler to a polymer matrix can greatly increase its stiffness, especially for thermoplastic materials in the rubbery region. However, thermosetting polymers have attracted far less attention, and much of the work that has been done using these materials has used elastomeric epoxies. Some studies have used rigid thermosets, though there have generally been no comparisons made between the properties of thermoset nano- and micro-composites. The present work presents such data, and will discuss how the morphology of the inorganic particles can affect the mechanical and fracture properties of the composites produced. This morphology is typically described as 'particulate' (or 'conventional'), 'intercalated' or 'exfoliated', as identified by wide-angle X-ray scattering (WAXS) [5, 6]. In an intercalated nano-composite, polymer chains enter the galleries and increase the measured spacing. For an exfoliated structure, the individual silicate layers (i.e. platelets) are pushed further apart, and the spacing becomes too large to measure using WAXS. For a particulate structure, the dimensions and structure of the particles essentially remain unchanged when introduced into the polymeric matrix.

2.2. Experimental

The epoxy used was a diglycidylether of bisphenol A/F, DGEBA/F, (AY105, Vantico, UK) cured using an amine hardener, polyoxypropylenediamine, (Jeffamine D230, Huntsman, USA). A range of inorganic particles was used, as shown in Table 2.1, comprising unmodified and organically-modified silicates. Sheets of epoxy composite, 6mm thick, were produced as follows. The epoxy was poured into a beaker, the inorganic particles were added and the mixture was stirred using a spatula. The beaker was placed in a vacuum oven at 75°C, and the entrapped air was removed. The vacuum was then released, and the mixture was left in the oven for 24 hours. After this time the mixture was stirred and a stoichiometric amount of hardener added. The mixture was stirred again and poured into a release-coated steel mould. The mould was placed in an oven, and the epoxy was cured for 3 hours at 75°C followed by 12 hours at 110°C [7]. The plate of epoxy was removed after cooling and machined to produce tensile dumbbell and fracture specimens according to the relevant standards. Note that the addition of the inorganic particles increased the viscosity of the epoxy resin, and hence there was a maximum concentration above which the viscosity of the resin was too high to be able to cast the sheets. For the Cloisite 30B and 25A modifiers, a maximum of 15% by weight could be used. The maximum addition of Nanomer I30E was 10%, and of Cloisite Na^+ was 20% by weight. For the mica-modified epoxy, 30% by weight could be used. The tensile specimens were tested at a constant displacement rate of 1mm/min, using an extensometer to measure the strain within the gauge length. The

fracture specimens were tested at a constant displacement rate of 1mm/min. Both compact tension and three-point bend tests were performed. The machined notch was sharpened by drawing a new razor blade across the notch tip prior to testing. (Note that the data produced were compared to data from specimens where a natural crack had been tapped into the specimen, and the K_c values using both techniques were found to be identical, within experimental error.) The glass transition temperatures of the samples were measured using differential scanning calorimetry (DSC), with a scan rate of 20°C/min.

Table 2.1: Silicate modifiers used in the present work, and the T_g and structure of the resulting epoxy composite.

Inorganic phase	Surface treatment	Platelet diameter	T_g, °C	Structure
None	None	-	78	-
Cloisite 25A	2MHTL8	10 μm	85	Intercalated
Cloisite 30B	MT2EtOT	10 μm	84	Intercalated
Cloisite Na^+	None	10 μm	81	Particulate
Mica R120	None	80 μm	80	Particulate
Nanomer I30E	Octadecylamine	10 μm	79	Exfoliated

Notes:

T_g and structure given for 10% by weight of silicate modifier.

Silicates are bentonite, except the mica R120.

2MHTL8: Dimethyl, hydrogenated tallow, 2-ethylhexyl quaternary ammonium.

MT2EtOT: Methyl, tallow, bis-2-hydroxyethyl, quaternary ammonium.

Cloisite clays supplied by Southern Clay Products, USA.

Nanomer I30E clay supplied by Nanocor, USA.

Mica R120 particles supplied by Microfine Minerals, USA.

2.3. Results

2.3.1. Introduction

The use of wide-angle X-ray scattering (WAXS) enabled the structure of the composites to be ascertained, i.e. whether they were exfoliated, intercalated or particulate in nature [8]. It was noteworthy that for the two intercalated nano-composites, that the 30B-modified composite had a higher d-spacing that the 25A-modified composite. These data are summarised in Table 2.1 in terms of the structure obtained. As may be seen, by changing the surface treatment, and hence the interfacial adhesion, the type of morphology obtained may be varied. Using scanning electron microscopy, the orientation of the particles was observed to be random in all cases.

2.3.2. Glass Transition Temperatures

The glass transition temperatures, T_g, for the epoxy polymer and the composites with 10% by weight of modifier are shown in Table 1. The unmodified epoxy has a T_g of 78°C. The values for the particulate and exfoliated composites lie within the range of 79±2°C. However, the intercalated composites show an increase in the value of T_g, to 84-85°C, caused by the additional constraint on the polymer chains within the galleries of the silicate. (Note that the data for the other concentrations of silicates show similar trends.)

2.3.3. Tensile Modulii

The measured tensile modulii increase with an increasing concentration of silicate modifier, see Figure 2.1. The coefficients of variation were typically ±5%. The largest increases in the modulii, at any given concentration of modifier, resulted from employing mica, which gave a particulate micro-composite, and the exfoliated clay nano-composite (i.e. prepared using the Nanomer I30E silicate). The other clay-modified materials showed only a relatively small increase in the measured modulus.

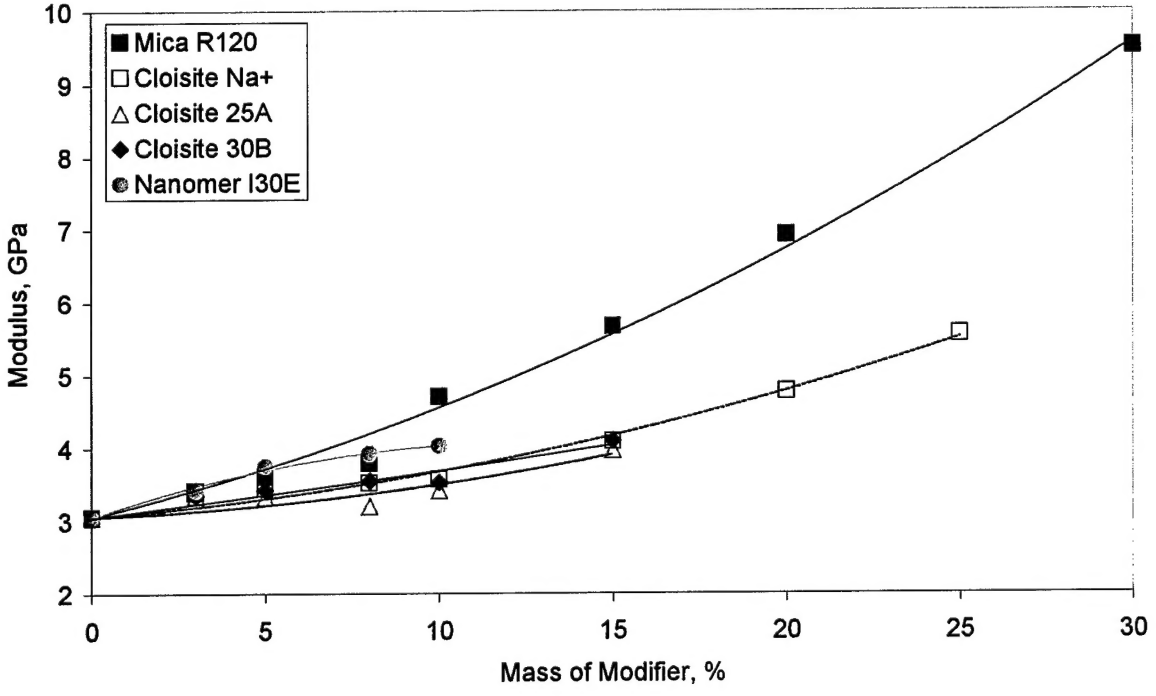

Figure 2.1: Tensile modulus of unmodified epoxy, micro- and nano-composites.

2.3.4. Fracture Toughness

A fracture toughness, K_c, value of 1.0MPam$^{1/2}$ was measured for the unmodified epoxy. This is a typical value for an unmodified thermosetting polymer in the glassy region [1]. A relatively large toughening effect was observed for the mica-modified epoxy, as shown in Figure 2.2. For example, a K_c value of 2.5MPam$^{1/2}$ was measured using 20% mica. This represents an increase of about 150% compared with the toughness of the unmodified epoxy. Previous work on this micro-composite has shown that this toughening effect is due to crack deflection and to plastic deformation being initiated around the particles, leading to the formation of cavities [9]. However, the epoxies modified with the surface-treated clay generally showed only a small toughening effect. Indeed, the maximum measured value of K_c was 1.7MPam$^{1/2}$, using 5% of the Cloisite Na^+ clay silicate.

Thus, for the clay-modified materials, the measured fracture toughnesses are lower than for the mica-modified epoxy. As the degree of exfoliation of the particles increases (i.e. for the composites modified with Cloisite Na^+ to 25A to 30B to I30E), then the toughness of the composite decreases, see Figure 2.2. It is suggested that, although the particles in the Nanomer I30E based nano-composite have exfoliated, the platelets may still retain their stacked-layer structure, i.e. they are not randomly distributed. In this case, they simply act like relatively larger particles, rather than as individual platelets. Hence, they effectively possess a somewhat lower aspect ratio, which leads to a relatively smaller toughening effect.

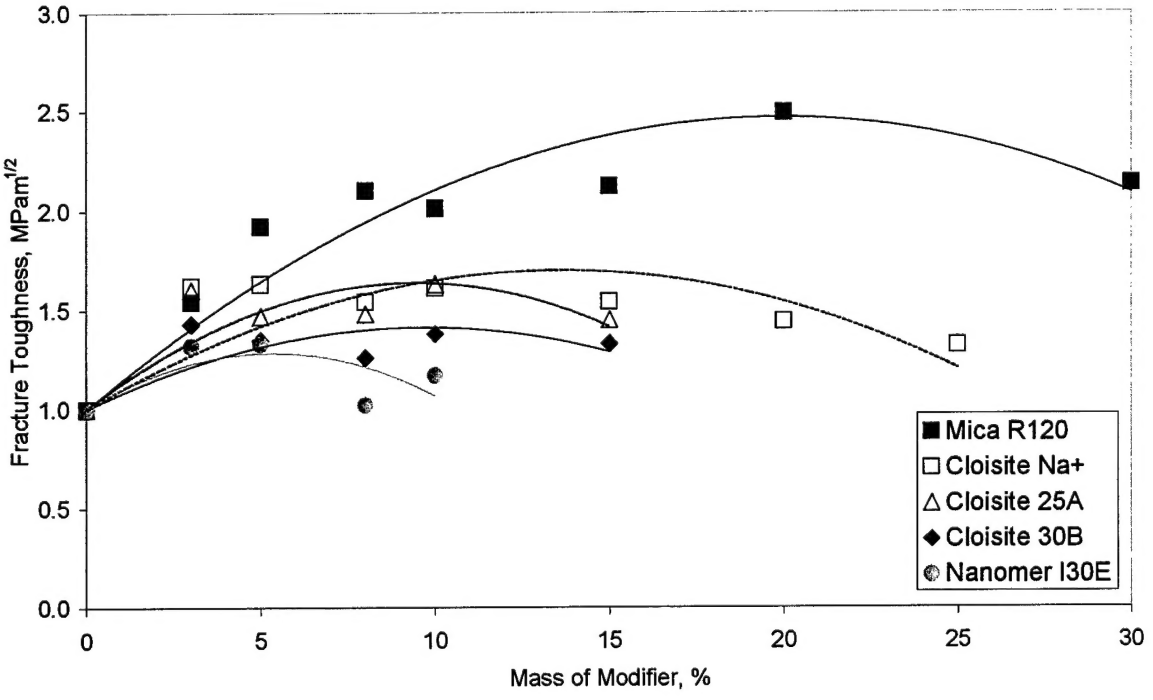

Figure 2.2: Fracture toughness of unmodified epoxy, micro- and nano-composites.

2.3.5. Modulus versus Fracture Toughness

The modulus values may be plotted versus the fracture toughness data to highlight which silicate modifier gives the most effective combination of properties, as shown in Figure 2.3. These data show that the mica-modified epoxy gives the greatest increase in both the fracture toughness and modulus. However, it should be noted that a maximum inclusion of 30% by weight of mica could be employed, compared with only 10 to 25% by weight being possible for the clay silicates. Nevertheless, even for the same percentage inclusion of modifier (e.g. 10%), the mica-modified epoxy micro-composite still shows the highest values of the fracture toughness and modulus.

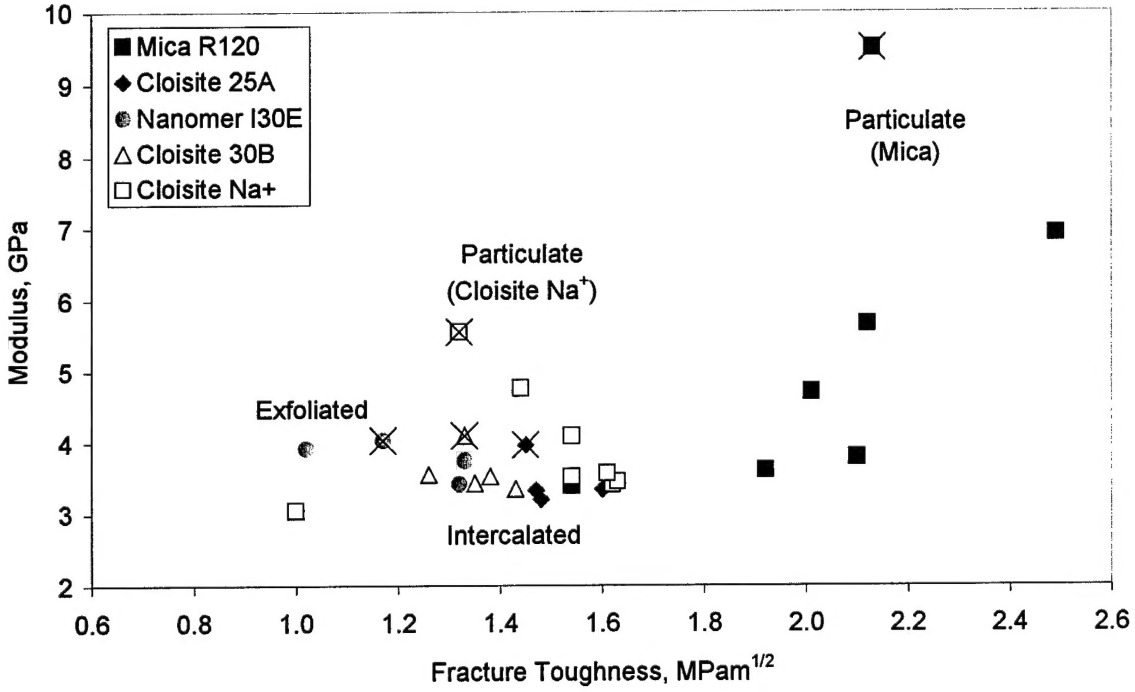

Figure 2.3: Tensile modulus versus fracture toughness of unmodified epoxy, micro- and nano-composites.

2.4. Comparison of Experimental with Theoretical Predictions

2.4.1. Experimental and Theoretical Modulus

There are many theoretical models that may be used to predict the modulii of particle-modified polymers, though amongst the most commonly used models are the Halpin-Tsai and the rule of mixtures relationships [10, 11].

However, the rule of mixtures provides an upper bound that is very rarely, if ever, achieved for these materials. Hence, the experimental data in the present work will be compared with the Halpin-Tsai predicted values. The Halpin-Tsai model gives the modulus of the composite, E_c, as a function of the modulus of the polymer, E_m, and of the modifier, E_f, as:

$$\frac{E_c}{E_m} = \frac{1 + \zeta \eta V_f}{1 - \eta V_f} \tag{2.1}$$

where ζ is the shape factor, V_f is the volume fraction, and:

$$\eta = \left(\frac{E_f}{E_m} - 1 \right) \Big/ \left(\frac{E_f}{E_m} - \zeta \right) \tag{2.2}$$

The volume fraction used in these predictions is the volume of the clay, without the modifier, because the model assumes that there is no organic surface-treatment on the silicate. (The surface-treatment will have a modulus approximately equal to, or less than, that of the epoxy. Hence, it does not stiffen the matrix, and thus only the volume of the silicate itself should be used.) Halpin and Tsai advise that the shape factor, ζ, may be taken to be 2w/t, where w/t is the aspect ratio of the particles. However, work by van Es [10] has shown that this value is too high for most particulate-modified polymers and he has recommended the use of $\zeta = 2w/3t$.

The predictions are compared to the experimental data in Figure 2.4, using an aspect ratio of w/t = 10. (The value of 10 was selected since the aspect ratio of the mica and clays prior to incorporation into the polymer is approximately 10, as determined by scanning electron microscopy.) Intercalation or exfoliation will affect the aspect ratio of the particles after incorporation. However, Figure 2.4 shows that there is apparently little effect of intercalation or exfoliation. Figure 2.4 also shows that the van-Es-modified Halpin-Tsai model predicts the modulii of these materials quite well. The mica-modified material tends to exhibit modulii that are slightly higher than the van Es prediction, whilst the clay-modified materials fall very close to the theoretical values.

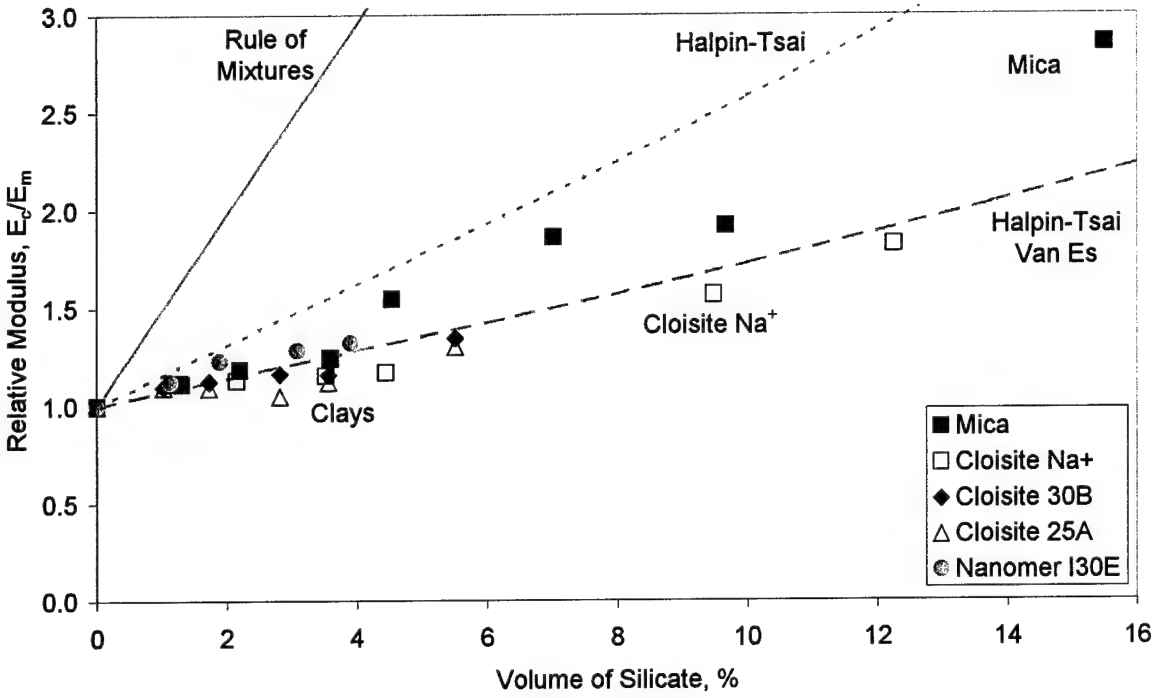

Figure 2.4: Relative modulus (composite modulus divided by epoxy modulus) versus volume percentage of silicate for micro- and nano-composites. Points are experimental data and lines are theoretical predictions using an aspect ratio of ten.

2.4.2. Experimental and Theoretical Fracture Energy

Kinloch and Taylor [9] have compared the toughening effect of particles in a polymer matrix to predictions using the Faber and Evans model [12]. In that work Kinloch and Taylor discussed particulate-modified thermosetting polymers in some detail. They used a range of silicate particles, including mica, and found good agreement between the predictions and the experimental data for small aspect ratios. However, the agreement was relatively poor when the particle aspect ratio was high. In these cases the model over-predicted the composite fracture energy.

In the present work, the fracture energy, G_c, of the composite samples can be calculated from the measured fracture toughness and modulus to allow comparison with the Faber and Evans predictions using:

$$G_c = \frac{K_c^2\left(1-\upsilon^2\right)}{E_c} \qquad (2.3)$$

where the Poisson's ratio $\upsilon = 0.4$. The calculated relative fracture energies, i.e. G_c of the composite divided by G_c of the unmodified epoxy, are shown in Figure 2.5, along with the Faber & Evans predictions for the toughening effect of platelets with aspect ratios of 12 and 3. For clarity, in this Figure second order

polynomial fits have been applied to the experimental data as a guide, and are shown as thin lines. These data show that the predicted values are much higher than the measured fracture energies. Indeed, most of the data lie below the prediction for an aspect ratio of 3, which is much lower than the true aspect ratio of the particles. Note that this analysis assumes that there is no effect of platelet size, but that the aspect ratio of the platelets is critical in determining the fracture energy of the composite.

The toughening effect predicted by Faber and Evans is due to a crack deflection mechanism. This requires a crack to be propagating through the specimen. However, in the present work the measured fracture energies are initiation values, and hence as a crack is not propagating, the crack deflection mechanism does not apply. Note that there is no orientation of the particles, unlike for adhesive joints [9], as scanning electron microscopy (SEM) showed that the particles were orientated randomly in the present work.

Even though crack deflection can be discounted, the particles would be expected to toughen the polymer by initiating plastic deformation, leading to the formation of cavities [9]. This will give a toughening effect, as occurs with the mica-modified epoxy. However, for the clay-modified materials, the measured fracture energies are lower than for the mica-modified epoxy, and there is little or no toughening effect. These particles are poorly bonded to the epoxy, and hence they may act as stress concentrations or micro-cracks at the tip of the crack. As the particles are so thin, especially in the case of the exfoliated platelets, their presence may effectively sharpen and lengthen the crack, leading to fracture at lower loads. Hence there is little toughening effect. The fracture energy would be expected to decrease when the volume fraction of particles increases as there will be a greater number of particles at the crack tip. Additionally, the exfoliated particles would be expected to give the lowest fracture energies, as these will give the sharpest defects. These effects are observed experimentally, see Figure 2.5.

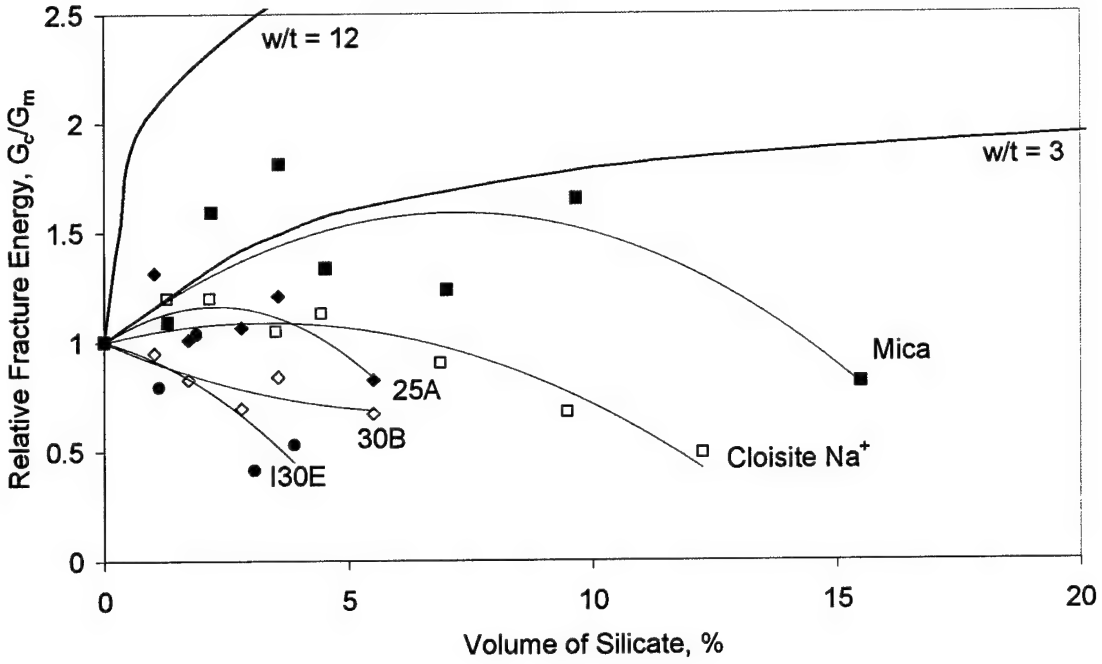

Figure 2.5: Relative fracture energy (composite fracture energy divided by epoxy fracture energy) versus volume percentage of silicate for micro- and nano-composites. Points are experimental data and bold lines are theoretical predictions using aspect ratios of 12 and 3.

2.5. Summary

Epoxy micro- and nano-composites have been manufactured using a range of inorganic modifiers, with exfoliated, intercalated and particulate morphologies; since, by changing the surface treatment, and hence the interfacial adhesion, the type of morphology obtained was be varied. The modulus and fracture toughness of these composites increased with the weight fraction of modifier. The fracture toughness was increased by up to 150% with the addition of mica, but the material modified with the surface-treated clays generally showed only a small toughening effect. Overall, the mica-modified epoxy showed the greatest increase in both stiffness and toughness. The modulii of the composites were in good agreement with predictions using the van-Es-modified Halpin-Tsai model. The fracture toughness of the clay-modified materials generally decreased as the degree of exfoliation increased, as the modifier acts like large particles rather than individual platelets, hence having a lower effective aspect ratio and a smaller toughening effect. The nanocomposites tend to behave in a similar manner to the microcomposites, and the same models can be applied to describe the performance of these systems.

3. Silica Nanoparticle and Rubber Toughening

3.1. Introduction

The highly crosslinked structure of thermosetting polymers leads to one highly undesirable property in that they are relatively brittle materials, with a poor resistance to crack initiation and growth. It has been well established [13-15] for many years that the incorporation of a second micro-phase of dispersed rubbery particles into the epoxy polymer can greatly increase their toughness, without significantly impairing the other desirable engineering properties. Typically the rubber particles are about 1 to 5 μm in diameter with a volume fraction of about 10 to 20%. However, the formation of a nano-phase structure in the polymeric adhesive, where the nano-phase consists of small rigid particles or fibres which have a diameter (or at least one dimension) of about 5 to 50 nm also holds great promise for increasing the mechanical performance of structural adhesives [8, 16]. The present work has combined these two approaches to developing improved structural adhesives with the aims of attaining relatively high toughness materials but without significantly compromising the other desirable mechanical and thermal properties of the adhesive.

3.2. Materials

The formulations were based upon a two-component epoxy adhesive system and the recipes are shown in Table 3.1. The epoxy resin was a standard diglycidyl ether of bis-phenol A (DGEBA) with an epoxy equivalent weight (EEW) of 185 g/mol, 'Bakelite EPR 164' supplied by Bakelite AG, Germany. 'Nanopox 22/0516' (Hanse Chemie, Germany) is a nano-particle silica (SiO_2) particle-reinforced bis-phenol A epoxy resin, which consists of surface-modified SiO_2 nano-particles with an average particle size of about 20 nm, and also with a narrow range of particle-size distribution. This particle size of about 20 nm is created during a sol-gel manufacturing process [17], whereby the silica particles are formed *in-situ*, and the particle size and excellent dispersion of these SiO_2 particles remain unchanged during any further mixing and/or blending operations. They were surface treated, by using an added silane-based coupling agent, to give excellent interfacial adhesion to the epoxy matrix. It is very noteworthy that, despite the relatively high SiO_2 content of 40% by mass, the nano-filled resin still has a comparatively low viscosity due to the agglomerate-free colloidal dispersion of the nano-particles of SiO_2 in the epoxy resin. The small diameter and good dispersion of the nano-particles of silica are clearly shown in Figure 3.1. The reactive liquid rubber, which give rises to the micrometer-sized spherical rubber particles upon curing of the adhesive formulation, was an amine-terminated butadiene-acrylonitrile rubber (ATBN). It was supplied by Noveon, USA, and was 'Hycar ATBN 1300x16' with an amine equivalent weight of 900 g/mol and acrylonitrile content of 18%. The curing agent was a hardener based upon a blend of N,N-dimethyl-1,3-diaminopropane and a polyaminoamide, namely 'Polypox P502' supplied by UPPC, Germany. The formulations were cured by firstly mixing together the two different epoxy-resin based components and, separately, the last two components given in Table 3.1 in the proportions, by mass, stated. Just prior to joint preparation and curing, these two blends were then mixed together, i.e. as Parts 'A' and 'B', respectively, of the two-component adhesive formulation. The adhesive was cured for 24 hours at room temperature followed by 2 hours at 60°C.

Table 3.1: Formulations of the two-part epoxy adhesives

	Control	2KA	2KB	2KC	2KD	2KE
DGEBA	100	96.25	92.5	85.0	70.0	-
Nanopox XP22/0516	-	6.25	12.5	25.0	50.0	100
Hycar ATBN 1300x16	45.8	45.2	44.5	43.9	43.2	27.8
Polypox P 502	91.6	90.4	88.9	87.9	86.5	55.5
% mass SiO_2 (on total)	*0*	*1.05*	*2.1*	*4.1*	*8*	*21.8*

Note: All formulations possess 18.1±1.5% on the total mass of ATBN.

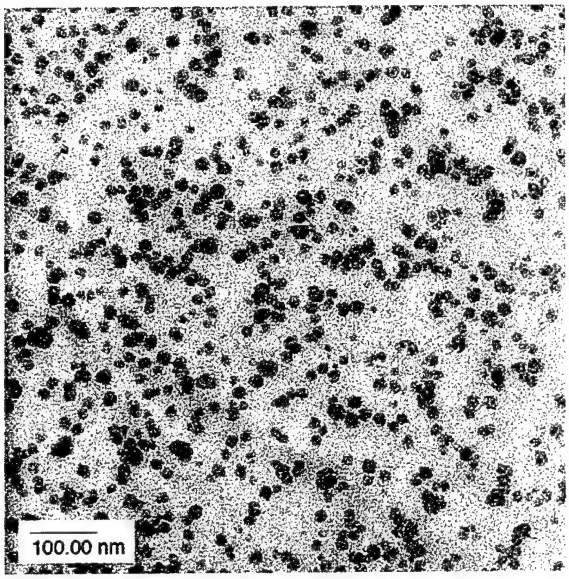

Figure 3.1: Transmission electron micrograph showing the excellent dispersion of the SiO_2 nano-particles in the epoxy resin ('Nanopox XP 22/0516').

3.3. Mechanical and Thermal Properties

The glass transition temperature, T_g, of the various formulations was measured using the method of dynamic mechanical thermal analysis (DMTA) at a frequency of 10Hz. The single-overlap shear strengths were determined using either untreated aluminium-alloy substrates (according to DIN Standard 55-283) or chromic-acid etched aluminium-alloy substrates (according to ASTM Standard 1002). The adhesive fracture energy, G_c, was measured using chromic-acid etched aluminium-alloy substrates and tapered double-cantilever beam (TDCB) specimens (according to BS Standard 7991). The coefficient of variation on the values of G_c was ±12%

3.4. Results

The results are given in Table 3.2. There are several noteworthy points. Firstly, the glass transition temperature, T_g, may be somewhat increased by the presence of the nano-silica particles. It would appear that a concentration of about 8% by mass of nano-SiO_2 particles results in an increase in the T_g by about 5°C, compared to the formulation containing no nano-SiO_2 particles.

Table 3.2. Mechanical and thermal properties of two-part epoxy with rubber particles and nano-SiO_2.

	Control	2KA	2KB	2KC	2KD	2KE
% mass SiO_2	0	1.05	2.1	4.1	8.0	21.8
T_g (°C)	70	67	71	67	75	73
Lap shear (1) (MPa)	13.4	19.2	17.8	16.7	16.2	11.8
Lap shear (2) (MPa)	20.8	20.9	22.0	23.0	23.2	20.3
G_c (J/m^2)	1200	1800	1800	2300	2000	1300

Notes:

a. Lap shear (1) tests used untreated aluminium-alloy.

b. Lap shear (2) tests used etched aluminium-alloy.

Secondly, however, far more striking is the increase in the value of the adhesive fracture energy, G_c, upon the addition of the nano-SiO_2 particles. The value of G_c increases from $1200J/m^2$ for the control rubber-toughened epoxy up to a maximum of $2300J/m^2$ for the formulation with an additional 4.1% by mass of nano-SiO_2 particles. Thus, there is clearly a very significant and substantial additional toughening effect induced by the additional presence of the nano-particles. Compared to the unmodified material with no dispersed rubbery phase, the rubbery particles are known to increase the toughness of the adhesive via interactions of the stress field ahead of the crack tip and the rubbery particles which leads to greatly enhanced plastic deformation of the epoxy matrix. It is not immediately obvious why the additional presence of the nano-SiO_2 particles should further increase the toughness so markedly. Previous work [9] on rigid fillers, but which were micrometres in size as opposed to be nanometres, has shown that the toughening mechanisms which are induced by the presence of the rigid particles may also involve enhancing the plastic deformation that occurs in the epoxy matrix, but that other mechanisms such as crack deflection and crack twisting [12] around the rigid particles may also be initiated. Future work will explore the detailed mechanisms of toughening which are initiated by the nano-particles, which may lead to even further increases in the mechanical performance of structural adhesives, containing a complex structure of nano- and micro-sized phase inclusions, being achieved.

Finally, the lap-shear strength was measured using single-lap joints loaded in tension. As indicated in Table 3.2, both untreated and chromic-acid etched aluminium alloys were used for the substrates. The use of the former type of substrate led to the lap joints failing mainly at the adhesive/substrates interface, whilst the use of the latter type of etched substrate led to failure occurring cohesively within the adhesive layer. The lap-joint strengths were considered to be of interest since an increase in the toughness of an adhesive material by a formulation change is often accompanied by a decrease in the lap-shear strength. However, clearly this is not the case with the nano-silica rubber-toughened materials. From Table 2 it is evident that the addition of the nano-SiO_2 particles to the rubber-toughened epoxy leads to a significant increase in the strength of the single-lap joints, prepared using either the untreated or the chromic-acid etched aluminium-alloy substrates.

3.5. Summary

It has been clearly demonstrated that the addition of low concentrations of nano-silica particles to a typical rubber-toughened adhesive, based upon a two-part epoxy formulation, leads to very significant increases in the toughness of the adhesive, and also to increases in the glass transition temperature and the single-lap shear strength. The nano-SiO_2 particles have an average particle diameter of 20 nm and are very well dispersed in the epoxy adhesive, and only a concentration of about 1% to 8 % by mass of such nano-particles are needed to achieve significant improvements in the mechanical and thermal performance of the rubber-toughened two-part epoxy adhesive.

4. Nanotube- and Nanofibre-Modified Epoxy Adhesives

4.1. Introduction

The toughening effect of carbon nanotubes and carbon nanofibres is being investigated using two different approaches. Firstly a preformed mat (either random or aligned) of nanotubes or nanofibres is impregnated with a low-viscosity epoxy resin. Secondly, a hot-melt formulation is used to allow extrusion of the resin prior to curing in order to investigate the effect of orientation under shearing on the properties of the thermoset polymer composites. Formulation of these systems has been time-consuming, as may be expected, but the viscosity and handleability of these systems is excellent for these applications.

4.2. Materials

4.2.1. Low-Viscosity Epoxy Resin

A low-viscosity resin has been formulated using a blend of epoxy resins comprising one backbone resin, one diluent and one anhydride curative, plus an advancement agent. A 100% solids formulation was prepared, as the difficulty in removing residual solvent from the nanotube or nanofibre mats precludes the use of a solution of the matrix in organic solvents. Various combinations of candidate resins were evaluated, considering the viscosity of the blend and the final glass transition temperature, as well as the stability of the blend during curing. The trifunctional Araldite CY 179 epoxy resin (Vantico, UK) was chosen to give the required low viscosity, but also the structural properties required for use as an adhesive. Araldite DY-T/CH (Vantico, UK) was used as a diluent at 30 parts by weight for every 100 parts of the CY 179, this being the maximum diluent loading that is commonly used in the formulation of structural adhesives. Due to the cycloaliphatic structure of CY 179, amine curatives cannot be used, and hence a liquid anhydride curing agent was chosen. Analysis of the trail formulations using dynamic differential scanning calorimetry (DSC) showed that a 100% stoichiometry of curing agent should be used, as an excess of anhydride retarded curing.

Initial trials without the use of an advancement agent showed that a significant amount of resin was lost during curing. Additionally, DSC analysis showed that the resin was not completely cured, indicating that the use of an advancement agent was essential with this combination of resins and curatives. The addition of the tertiary amine advancement agent, dimethyl benzylamine, at a stoichiometry of 5 or 10% gave full cure. As there was little difference between the DSC data using these two levels of loading, a stoichiometry of 7.5% was chosen for the final formulation, as shown in Table 4.1. To characterise the cure of this final formulation, further dynamic and isothermal DSC analyses were performed on the system. These indicated that curing was possible at 120°C, though the use of a temperature as low as 100°C may be possible. To optimise the thermal performance, and increase the value of the glass transition temperature, post-curing at higher temperatures can be performed.

Table 4.1: Low-viscosity epoxy formulation.

	pbw	%
Araldite CY 179	100.0	35.65
Araldite DY-T/CH	30.0	10.69
Lindride 52D	148.9	53.09
Dimethyl Benzylamine	1.6	0.57
Total	**280.5**	**100.00**

4.2.2. Hot-Melt Epoxy Resin

A hot-melt formulation will be used to allow extrusion of the resin prior to curing in order to investigate the effect of orientation under shearing on the properties of the thermoset polymer composites. This part of the project requires a formulation comprising reactive systems which were solid at ambient temperature but which would pass into a liquid state at about 80°C, so that conventional film adhesives manufacturing technology could be employed, before curing in the region of 175°C. It was found that specialist mixing equipment was required to achieve a good blend. Hence a dual axis centrifugal mixer (FlackTek SpeedMixer, UK) was purchased and commissioned.

The initial trials clearly showed that the Tactix 742 (Dow, USA) resin was of too low molecular weight to act as a perfect film former. Hence a significant loading of a suitable, Bisphenol A solid epoxy resin was incorporated into the basic matrix, to ensure that a good film was produced; i.e. one which was both flexible and relatively tack-free. The preferred choice was DER 668 (Dow USA), whose softening point is quoted as 130° to 140°C, which means that the real melting point will be in the region of 160°C. Thus formulating trials used simple blends of Tactix 742, DER 668 and DER 332. DER 332 was chosen as it is generally the preferred liquid resin for structural adhesive use, and due to its high purity it is liable to give a more controlled curing reaction.

Blends were prepared using the centrifugal mixer to obtain a homogeneous mixture. It was found that the order of addition of material to the mixing pot is important; liquid materials should be charged before solid material. Further, the liquid resin loading, when dissolving the solid resins, should be kept at as low a level as possible. The trials indicated that the liquid level should probably not fall below about 14% of the total and there was some evidence that the upper level should be in the region of 45 to 50%. Homogeneous mixing, for a formulation containing materials of widely disparate molecular weights and melting/softening points, was only achievable by master-batching the highest molecular weight materials with some of the most liquid. Insoluble powders aid the production of good solutions/dispersions; the curatives and the carbon nanotubes/nanofibres should be added together with the master-batch and the solid resins.

It was found that the most successful way to prepare this formulation was to prepare a DER332/DER668 master-batch, see Table 4.2. The master-batch was blended, then frozen for two hours at -18°C and was then broken up into flakes for incorporation into the final blend. The robustness and reproducibility of the mixing technique was found to be good. The final formulation is shown in Table 4.3. The film produced by casting the resin matrix at about 70°C onto PTFE sheet was very handleable and of relatively low tack after cooling to room temperature.

Dynamic and isothermal DSC analyses were then carried out to characterise the reaction kinetics of this formulation. Both dicyandiamide and DDS (4-4'-diamino diphenyl sulfone) were evaluated as curing agents, on their own and as a blend. However, the addition of DDS gave no advantages, and hence the simpler dicyandiamide system was chosen using an 85% stoichiometry. However, the use of dicyandiamide from Sigma-Aldrich, UK, gave a large exotherm during curing, so the final formulation will use dicyandiamide with a larger particle size (Dyhard 100 from Degussa), which will reduce the size of the exotherm. Isothermal DSC showed that this system could be cured at 175°C, and if necessary a step cure of 150°C followed by 175°C can be used.

Table 4.2: Masterbatch for hot-melt epoxy formulation.

	pbw	**%**
DER 332	50.0	33.33
DER 668	100.0	66.67
Total	**150.0**	**100.00**

Table 4.3: Hot-melt epoxy formulation with 2% by mass of carbon nanofibres.

	pbw	**%**
DER 332	75.0	27.28
Tactix 742	100.0	36.37
DER 668 Masterbatch	75.0	27.28
Dicyandiamide	19.4	7.07
Carbon Nanofibres	5.5	2.00
Totals	**274.9**	**100.00**

4.3 Results

Tapered double-cantilever beam (TDCB) specimens were prepared using the hot-melt epoxy formulation and tested according to the relevant standard (BS ISO 13586). A chromic-sulphuric acid etch surface treatment was used prior to bonding to ensure that failure occurred cohesively within the adhesive. The epoxy was heated to 80°C and spread on the surface of the beams. The beams were placed in a jig, light pressure was applied, and the epoxy was cured for 2½ hours at 175°C. The specimens were tested at a constant displacement rate of 1 mm/min, with load, displacement and crack length data being recorded. These data were analysed to give values of the fracture energy, G_c. These initial trials used three formulations – the unmodified epoxy, the epoxy with 2% carbon nanofibres as shown in Table 4.3, and the epoxy with 2% multi-walled carbon nanotubes.

All the formulations tested failed by unstable crack growth in a stick/slip manner, as is common for relatively brittle epoxies. Where unstable failure occurs, the Appendix to the standard (BS ISO 13586) recommends that the mean initiation values of the fracture energy should be quoted. In the present work a mean initiation fracture energy of 130 J/m^2 was measured for the unmodified epoxy, as shown in Table 4.4. The addition of 2% by mass of multi-walled carbon nanotubes gave a 13% increase in the mean initiation fracture energy, but this lies close to the experimental scatter of 5 to 10%, and hence may not be significant. The carbon nanofibres do give a significant toughening effect, the mean initiation value of G_c increasing by 25% to 160 J/m^2.

Table 4.4: Fracture energies, G_c, for hot-melt epoxy formulations.

	Gc, J/m^2	Increase, %
Unmodified	130	-
2% carbon nanotubes	145	13
2% carbon nanofibres	160	25

The observed toughening effect of the carbon nanofibres is comparable to that observed for the plate-like silicate modifiers discussed earlier, as an equal volume of modifier gives a similar increase in fracture energy. However, as the carbon nanofibres have a lower density than the silicates, then the nanofibres give a greater toughening when an equal percentage by weight is used. The measured fracture energies can be compared to predictions by Faber and Evans for the toughening effect of rod-like particles in a polymer [12]. The experimental values lie below the theoretical predictions, so the toughening effect is not as large as expected. However, the effect of orientation must be considered. The model assumes that the nanofibres are randomly oriented, whereas in these adhesive joint specimens they are oriented parallel to the substrates. Hence we would expect the toughening effect to be greatly reduced, as is observed.

Inspection of the fracture surfaces of the specimens with 2% carbon nanofibres using scanning electron microscopy shows nanofibres that have pulled out of the epoxy matrix, see Figure 4.1. Shorter broken nanofibres are also observed. This indicates that the nanofibres are indeed involved in the fracture process.

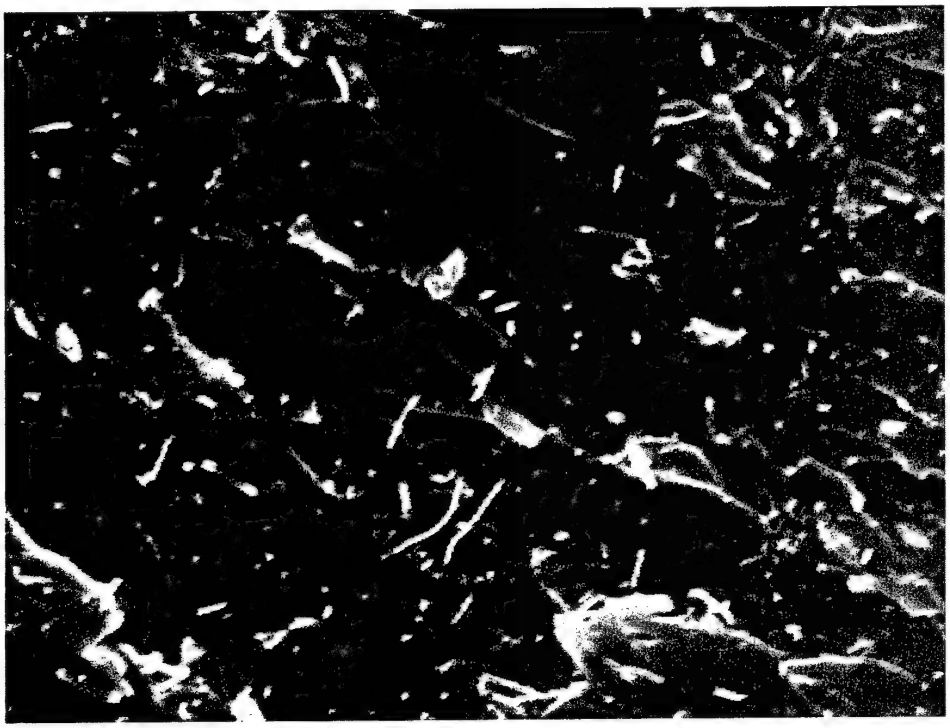

Figure 4.1: Scanning electron micrograph of fracture surface of epoxy with 2% carbon nanofibres.

4.4 Summary

Two structural epoxy adhesives have been formulated to investigate the toughening effect of carbon nanotubes and nanofibres. These are a low-viscosity resin and a hot-melt formulation. The viscosity and handleability of these formulated systems is excellent. The addition of 2% by mass of multi-walled carbon nanotubes to the hot-melt epoxy gave no significant increase in the mean initiation fracture energy, but the carbon nanofibres do give a significant toughening effect, the mean initiation value of G_c increasing by 25% to 160 J/m^2.

5. Finite Element Modelling of Particulate Composites

5.1. Introduction

The toughness of the brittle epoxy polymers (matrix) used as a basis for structural adhesives can be improved by the addition of a particulate phase at a micro- or nano scale [1, 16]. The resultant adhesive is no longer a homogenous material and the mechanical behaviour of these micro- or nanocomposites needs special treatment. In addition, due to the difference between the stiffness of the particulates and of the matrix, the induced deformation under loading can result in a wide distribution of stresses and strains within each of the components. It is expected that although the particulates undergo small strains, most of the strain will accumulate within the matrix. This work discusses two different ways of modelling these kinds of composites using finite element method. These are:

- Image-Based Unit Cell (IBUC) Model.
- Uniform Idealised Unit Cell (UIUC) Model.

The methodologies in this paper have been verified by applying these two methods to an epoxy adhesive filled with various volume fractions (V_f) of hollow, spherical, glass beads with diameter range of 2-30 μm with a mean diameter of 11.7 μm.

5.2. Image-Based Unit Cell (IBUC) Model

In this method, advances in imaging techniques are applied to understand the distribution of particulates in an epoxy matrix. The objective is to determine the strain distribution within the matrix using digitised images analysed with finite element procedures. This approach captures the image of the specimen cross-section and converts this image into a finite element mesh after image processing. The finite element program ABAQUS [18] provides numerical solutions to relate the average mechanical behaviour of the composites to stresses and strains within its domains. In this method, a real digitised image of the composite structure is prepared from a scanning electron microscope (SEM) image. An area of the SEM picture (the unit cell) is chosen such that it is representative of the bulk composite. Initially the original SEM image of the unit cell is converted into a high contrast binary image which is either white or non-white in colour, see Figure 5.1.

The binary unit cell image is then digitised to an ASCII format by a program based on MATLAB software that distinguishes the white and non-white zones of the binary image. In this format information about the numbers of pixel in both vertical and horizontal directions, the actual size of the image and the centre coordinate of each pixel becomes available. A mesh is designed and mapped over the image as shown in Figure 5.2. A user subroutine based on ABAQUS finite element software is then employed to call the integration points on each element and assign the relevant material properties to these integration points according to the properties of the materials which constitute the composites. For example in Figure 5.2, the properties of the glass were assigned to the integration points of each element in the white area while the

properties of the epoxy were assigned to the integration points in the black area. In the analysis, the white and non-white areas represent each material in the composite. Figure 5.3 shows the contour plot of the field variable output from ABAQUS. Three different colours represent the pure epoxy elements (black); the pure glass bead elements (dark grey) and the mixed epoxy/glass bead elements (light grey). It can be seen that this contour plot is a representative picture of the real composite microstructure. Since maximising the number of integration points on each element increases the accuracy of the results, elements with full integration are preferred to the reduced integration type. Mesh sensitivity analysis was performed to find the required level of mesh refinement. All simulations were performed with ABAQUS [18].

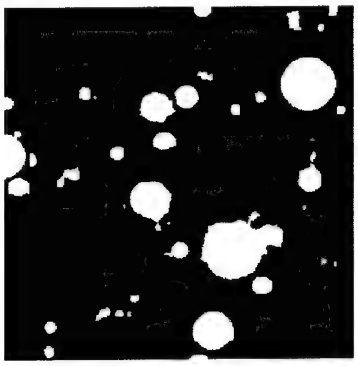

Figure 5.1: Binary image of glass bead-epoxy composite unit cell (V_f=10%) used in the FEA.

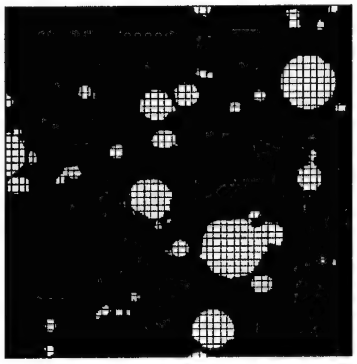

Figure 5.2: The image with the mapped finite-element mesh.

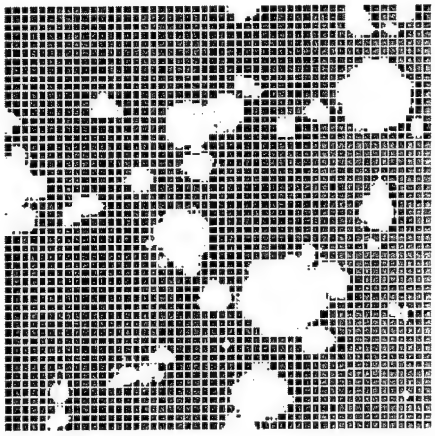

Figure 5.3: Material properties in the model. Black: epoxy, Dark grey: Glass beads, Light grey: Mixed elements

Since the unit cell is a representative piece of the bulk material, its behaviour must be repetitive in both horizontal and vertical directions. Hence, the appropriate boundary conditions on the edges of the unit cell are periodic boundary conditions when loading along each direction. The uniaxial tensile loading was imposed by applying the appropriate displacement boundary condition along each of the orthogonal directions. The macroscopic stress was then obtained from the force-displacement curve obtained from the FEA results. Finite element analyses of uniaxial loading of glass-epoxy composites were performed using the above procedure. Three different volume fractions of glass beads, of 10%, 20% and 30%, were modelled. In addition, tensile dumbbell specimens were manufactured using these volume fractions and tested in uniaxial tension at a displacement rate of 1mm/min.

The finite element predictions of the accumulated plastic strain under uniaxial tensile loading along the x-direction for glass-epoxy composite with V_f=10% are shown in Figure 5.4. The formation of shear bands across the unit cell is clearly visible. By imposing this shear band on the original micrograph (see Figure 5.1), it was found that the shear band passed between the glass beads. Also, the contour plot of the tensile stresses (σ_{xx}) under uniaxial tensile loading along the x-direction for glass-epoxy composite with V_f=10% is shown in Figure 5.5. A non-uniform distribution of tensile stress occurs across the unit cell with its maximum over the glass beads.

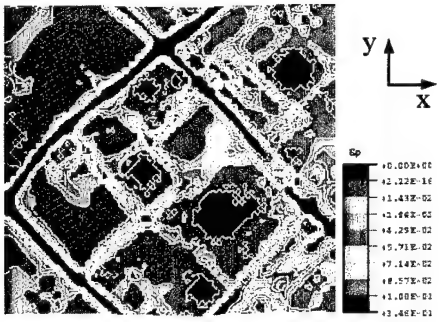

Figure 5.4: Contour plot of accumulated plastic strain under uniaxial tensile loading along the x-direction for glass-epoxy composite with V_f=10%.

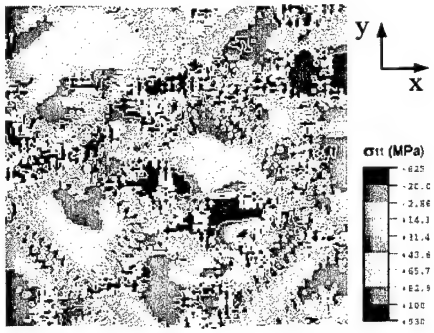

Figure 5.5: Contour plot of tensile stress (σ_{xx}) under uniaxial tensile loading along the x-direction for glass-epoxy composite with V_f=10%.

The IBUC model was initially verified by modelling the homogenous unmodified epoxy. In this case, the experimental results and the IBUC model match each other as shown in Figure 5.6. Next, the predictions of the stress-strain behaviour of the glass-epoxy composite with a volume fraction of 10% glass obtained from the IBUC model were compared with those from experiments. The results for the glass-epoxy composite model are very close to the experimental data. The observed slight difference is due to either a small

discrepancy between the exact match of the unit cell properties and the bulk of the composite, and/or the detachment of the glass beads from epoxy in the experiment. In the model, the bond was assumed to be perfect and remained so throughout the loading process.

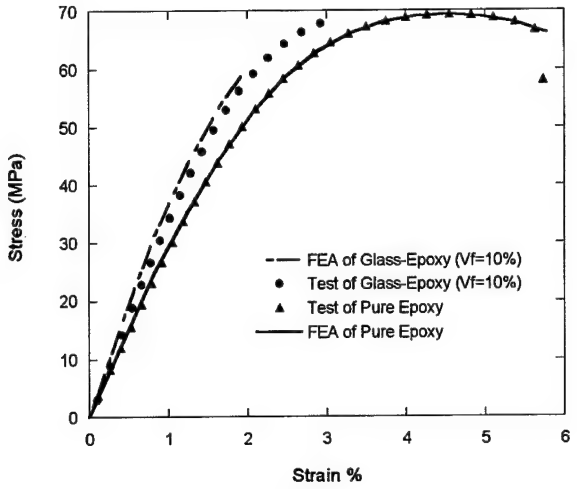

Figure 5.6: Comparison of stress-strain response obtained from the digitised image unit cell model (IBUC) analyses of the glass-epoxy composite with experimental data, for V_f=10%.

5.3. Uniform Idealised Unit Cell (UIUC) Model

In this model, a unit cell is artificially designed using an appropriate volume fraction of glass beads in the unit cell. The particulates are assumed to be cylindrical, all having the same diameter, and to be dispersed uniformly throughout the composite. A sample of this model of unit cell is shown in Figure 5.7.

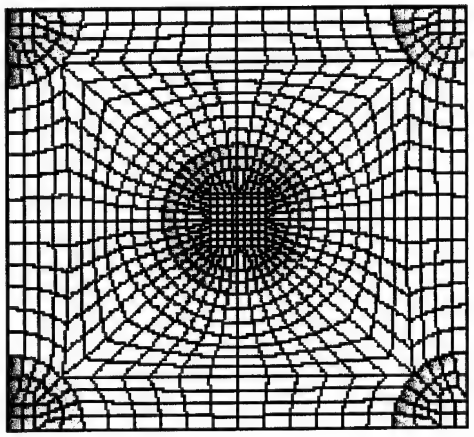

Figure 5.7: Uniform Idealised Unit Cell (UIUC) model, V_f=20%.

A quarter of particulate was put at each corner of the cell to enable the interaction between the particulates to be modelled. The advantage of this model is the ability to debond either parts of or the whole

of the central particulate from the matrix. Note that the four quarter particulates were assumed to be perfectly bonded to the matrix and remain so throughout the loading process.

Five different scenarios of debonding the glass bead at the centre of the unit cell from the epoxy matrix were envisaged. These were (a) complete attachment, (b) detachment of two opposite quarters, (c) half-perimeter detachment, (d) complete detachment (in these four cases periodic boundary conditions were applied) and (e) complete detachment where non-periodic boundary conditions were applied. The deformed shapes of the FE analysis of these cases are shown in Figure 5.8 (a)-(e).

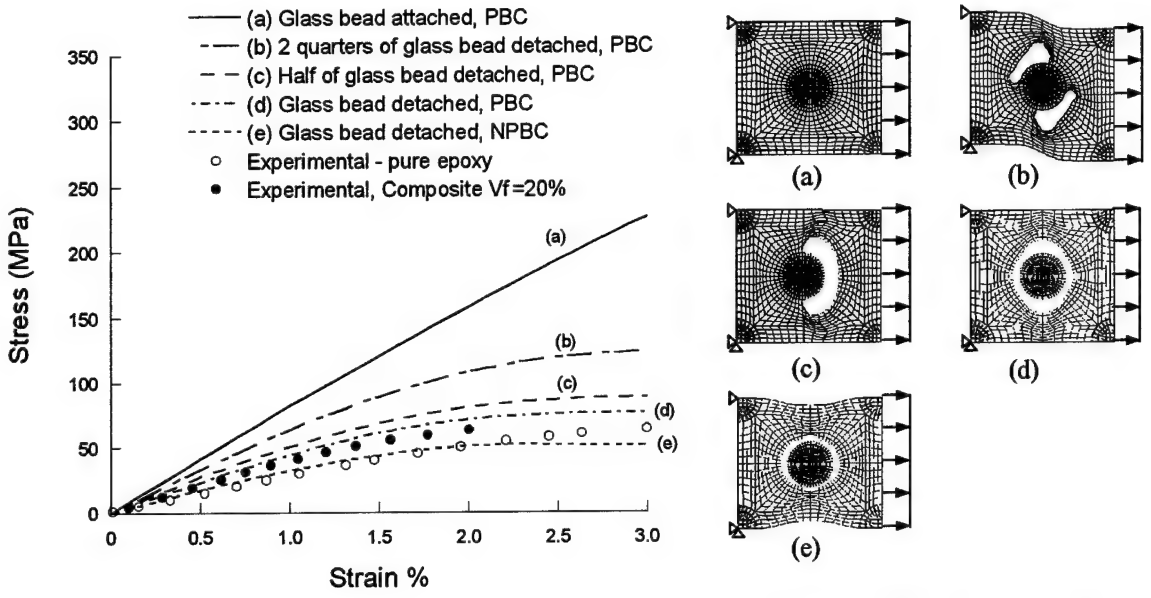

Figure 5.8: Stress-strain curves of epoxy-glass beads composites, V_f =20%. PBC ≡ periodic boundary conditions, NPBC ≡ non-periodic boundary conditions. Figures a-e show the deformed shape of the uniform idealised unit cells with various parts of the glass beads debonded.

The stress-strain response of all the different cases are shown and compared with the experimental results of epoxy-glass bead composites with a volume fraction of 20% in Figure 5.8. The experimental results are very close to case (d) where the glass beads are completely detached from the epoxy matrix while the periodic boundary condition were applied. This confirms the experimental observations that there is little or no adhesion between the glass and the epoxy matrix.

5.4. Summary

Two different ways of modelling particulate composites using the finite element method have been investigated. These are the Image-Based Unit Cell (IBUC) and the Uniform Idealised Unit Cell (UIUC) model. The methodologies have been verified by applying these methods to an epoxy adhesive filled with various volume fractions (V_f) of hollow glass spheres. The agreement between the theoretical predictions of the stress versus strain response and the experimental data is good. The IBUC model allows the true microstructure of the composite to be used in the theoretical predictions, and agreement between the predictions and the experiments is very close. The model also predicts the formation of shear bands within the epoxy matrix. For the UIUC model, the experimental results are very close to the case where the glass beads are completely detached from the epoxy matrix, with periodic boundary conditions. This confirms the experimental observations that there is little or no adhesion between the glass particles and the epoxy matrix.

6. Future Work

The work to date has shown how the mechanical and fracture properties vary with the microstructure of the epoxy composite [8, 19]. The use of nano-modifiers can give significant increases in the mechanical and fracture properties of thermosetting epoxies. In addition, it has been demonstrated that the mechanical response of these materials can be predicted using finite-element modelling [20].

There is, however, further work required to investigate some of the observed effects. In addition, the effect of particle orientation, the formation of multiphase materials, and modelling the performance of nanocomposites should be investigated. The main aims of any future work should be:

- To produce polymer-matrix composites with various nano-sized modifiers, including carbon nanotubes, nanofibres and nano-mats. The formulation studies described in the present report have laid the foundation for this work.
- To characterise the structure and mechanical properties of these composites, especially the fracture performance.
- To investigate the effect of orientation of the modifiers within the polymer matrix. Again, the formulation studies described in the present report have laid the foundation for this work.
- To undertake quantitative modelling studies to predict the performance of the composites. These studies will build upon the initial work on the analytical and computational models described above. For example, the finite-element analysis computational models described above have been validated so far by comparison with experimental data from micrometer-sized particles, clearly the next step is to model and validate against nano-sized modifiers.

7. Conclusions

Epoxy micro- and nano-composites have been manufactured using a range of inorganic-silicate modifiers, with exfoliated, intercalated and particulate morphologies being obtained. Indeed, by changing the surface treatment, and hence the interfacial adhesion, the type of morphology obtained could be varied. The modulus and fracture toughness of these composites increased with the weight fraction of modifier. The fracture toughness was increased by up to 150% with the addition of mica, which gave a classic micro-composite particulate material. However, when the epoxy was modified using the clay-silicates, then generally only a relatively small toughening effect was observed, and the fracture toughness of the clay-modified materials generally decreased as the degree of exfoliation of the clay particles increased. Indeed, overall, the mica-modified epoxy micro-composite showed the greatest increase in both stiffness and toughness compared with the unmodified thermosetting epoxy polymer. The modulii of the both the micro- and the nano-composites were in good agreement with predictions using the van-Es-modified Halpin-Tsai model. The fracture toughness of the clay-modified materials generally decreased as the degree of exfoliation increased, as the modifier acts like large particles rather than individual platelets, hence having a lower effective aspect ratio and a smaller toughening effect. The nanocomposites tend to behave in a similar manner to the microcomposites, and the same models can be applied to describe the performance of these systems.

It has been clearly demonstrated that the addition of low concentrations of nano-silica particles to a typical rubber-toughened adhesive, based upon a two-part epoxy formulation, leads to very significant increases in the toughness of the adhesive and also to increases in the glass transition temperature and the single-overlap shear strength. The nano-SiO_2 particles have an average particle diameter of 20 nm and are very well dispersed in the epoxy adhesive. They were surface treated, by using an added silane-based coupling agent, to give excellent interfacial adhesion to the epoxy matrix. A concentration of only about 1% to 8 % by mass of such nano-particles are needed to achieve significant improvements in the mechanical and thermal performance of the rubber-toughened two-part epoxy adhesive. These novel results represent the first report of nano-particles significantly increasing the toughness of thermosetting polymers.

Two structural epoxy adhesives have been formulated to investigate the toughening effect of carbon nanotubes and nanofibres. These are a low-viscosity resin and a hot-melt formulation. The viscosity and handleability of these formulated systems is excellent. The addition of 2% by mass of multi-walled carbon nanotubes to the hot-melt epoxy gave no significant increase in the mean initiation fracture energy, but the carbon nanofibres do give a significant toughening effect, the mean initiation value of G_c increasing by 25% to 160 J/m^2.

Two different methods for modelling particulate composites using the finite element method have been investigated. These are the Image-Based Unit Cell (IBUC) and the Uniform Idealised Unit Cell (UIUC) models. The methodologies have been initially verified by applying these methods to an epoxy adhesive

filled with various volume fractions of hollow, spherical, glass beads. The agreement between the theoretical predictions of the stress versus strain response and the experimental data is good. The IBUC model allows the true microstructure of the composite to be used in the theoretical predictions, and agreement between the predictions and the experiments is very close. The model also predicts the formation of shear bands within the epoxy matrix. For the UIUC model, the experimental results are very close to the case where the glass beads are completely detached from the epoxy matrix, with periodic boundary conditions. This confirms the experimental observations that there is little, or no, adhesion between the hollow glass spheres and the epoxy matrix.

8. Acknowledgements

The authors would wish to acknowledge the assistance of D. H. Hadavinia and Mr. J.H. Lee.

References

1. A.J. Kinloch, Adhesion and Adhesives : Science and Technology, 1987, Chapman & Hall, London.
2. A.J. Kinloch, *Proceedings of the Institution of Mechanical Engineers*, 1997, 211, pp 307-.
3. A. Usuki, et al., *Journal of Materials Research*, 1993, 8, pp 1179-1184.
4. M. Alexandre and P. Dubois, *Materials Science and Engineering, R: Reports*, 2000, 28, pp 1-63.
5. R.A. Vaia, in Polymer-Clay Nanocomposites, T.J. Pinnavaia and G.W. Beall, Editors, 2001, John Wiley & Sons, Chichester, pp 229-266.
6. R.A. Vaia and E.P. Giannelis, *Macromolecules*, 1997, 30, pp 8000 -8009.
7. X. Kornmann, H. Lindberg, and L.A. Berglund, *Polymer*, 2001, 42, pp 4493-4499.
8. A.J. Kinloch and A.C. Taylor, *Journal Of Materials Science Letters*, To be published.
9. A.J. Kinloch and A.C. Taylor, *Journal of Materials Science*, 2002, 37, pp 433-460.
10. M. vanEs, in *Nanocomposites 2000*, 2000, Brussels, Belgium, Emap Maclaren.
11. J.C. Halpin and N.J. Pagano, *Journal of Composite Materials*, 1969, 3, pp 720-724.
12. K.T. Faber and A.G. Evans, *Acta Metallurgica*, 1983, 31, pp 565-576.
13. A.J. Kinloch, et al., *Polymer*, 1983, 24, pp 1341-1354.
14. R.S. Drake and A.R. Siebert, *SAMPE Quarterly*, 1975, 6, pp 11-.
15. E.H. Rowe, A.R. Siebert, and R.S. Drake, *Modern Plastics*, 1970, 49, pp 110-.
16. A.J. Kinloch and A.C. Taylor, *Journal of Materials Science*, 2003, 38, pp 65-79.
17. S. Sprenger, et al., *Adhaesion, Kleben & Dichten*, 2003.
18. Abaqus User's Manual Version 5.8., 1998, Habbitt Karlsson and Sorensen Inc., Providence, RI, USA.
19. A.C. Taylor, A.J. Kinloch, and A.E. Tarrant, in *26th Annual Meeting*, 2003, Myrtle Beach, USA, The Adhesion Society, Blacksburg, USA.
20. A.C. Taylor, H. Hadavinia, and A.J. Kinloch, in *Yield, Deformation & Fracture of Polymers*, 2003, Cambridge, Institute of Materials, London.